

Copyright 2000, Society of Photo-Optical Instrumentation Engineers

This paper was published in Optical Microlithography XIII, Volume 4000 and is made available as an electronic reprint with permission of SPIE. One print or electronic copy may be made for personal use only. Systematic or multiple reproduction, distribution to multiple locations via electronic or other means, duplication of any material in this paper for a fee or for commercial purposes, or modification of the content of the paper are prohibited.

# High transmission attenuated PSM – Benefits and Limitations through a validation study of 33%, 20% and 6% transmission masks

Nishrin Kachwala\*, John S. Petersen\*\*, Martin McCallum\*

Nishrin.Kachwala@sematech.org

\*International Sematech, 2706 Montopolis Drive, Austin, TX 78741

\*\*Petersen Advanced Lithography, P.O. Box 162712 Austin, TX 78716

## ABSTRACT

Simulations indicate high transmission attenuated phase shift mask to improve resolution, reduce line end shortening, corner rounding and provide process window enhancements for some pitches. They also indicate that as the transmission is increased for line features, the Normalized image log slope (NILS) increases for all pitches. In this work the performance of 33% and 20% attenuated masks has been compared against 6% and binary masks.

Imaging results were obtained for 160nm features at various pitches with a 0.6NA 248nm SVGL MSIII with conventional and annular illumination. Performance of high transmission in terms of Depth of Focus, Overlapping process windows (ODOF), Exposure latitude and Proximity effects with the various % transmissions. Critical issues such as manufacturing of tri-tone masks, Inspection, Repair and material availability for High transmission (HiT) masks will be addressed.

## INTRODUCTION

For gate level lithography Alternating PSM (alt. PSM) is a popular choice for features below 160nm with 248nm lithography. However for certain applications, the layout of Alternate phase shifted and unshifted structures can be complicated and require double exposure to get rid of phase edges. From literature (1) it is known that low transmission (5-6%) attenuated PSM (att. PSM) provide a benefit for gate type structures with off-axis illumination. High transmission attenuated PSM can provide as much resolution and Depth of Focus (DOF) as an alternating PSM (2), except for MEF. Also layout and fabrication of an att. PSM is simpler than an alt. PSM. Simulations have indicated that, high transmission masks provide benefits over the conventional transmission ones in terms of resolution, DOF, better pattern fidelity through focus i.e. reduced corner rounding and line end shortening (3). The goal of this work was to establish the benefits of HiT att. PSM and study limitations if any.

## 1. Experimental conditions:

160nm line/space features with no OPC correction were imaged with duty cycles 1:1, 1:1.25, 1:1.5, 1:2, 1:2.5, 1:3, 1:5 and 1:10. Bare silicon wafers were coated with 0.450 $\mu$ m resist M20G (JSR) and UV6 (Shipley) on 60nm DUV-30 (Brewer Science) BARC. Softbake 140°/60sec for M20G and 130°/60 for UV6 and Post exposure bake was 130°/90sec. A 248nm SVGL MSIII scanner with a 0.6NA and 0.8 $\sigma$  conventional illumination and a 0.6 inner sigma and 0.8 outer sigma for the annulus was used. CD measurements and Profiles were made using a KL8100 CD SEM and Hitachi cross-section SEM respectively. Process windows were derived using PRODATA from Finle Technologies.

## 2. Reticles :

The attenuated material for the 6% and 33% was MoSi, and for the 20% was Cr/CrF. All three masks are tri-tone; i.e. MoSi had chrome over it in some areas (Figure 1 and 3). Simulations indicated that features only above 300nm would require chrome shielding as too much light through the leaky material would otherwise degrade its performance. Blanks coated with films with transmissions above 5-6% are not readily available, as they are not yet in production. To achieve higher transmission masks without developing new blanks a 6% attenuated material was used. Using Matrix theory for analysis of multilayer systems (4), the transmission can be tuned by varying the optical properties and thickness of the thin film layers, assuming that the incident radiation angle and  $\lambda$  are fixed. For a fixed n (refractive index) and k (extinction coefficient) of the 6% material, by reducing the thickness of the MoSi, the transmission through the film can be increased. The  $\pi$  phase difference for optical interference was adjusted by etching into the quartz (Figure 2).

### 3. Imaging results:

#### 3.1. Conventional Illumination 0.6NA, 0.8σ

For conventional illumination lower coherence was chosen based on simulations and some verification with imaging. For on-axis the illumination sigma could modulate the CD when with high %Transmission. The weak shifter like the binary mask does have zero diffraction order in the lens pupil. Thus the NA and partial coherence were optimized in the same way as typically done for binary chrome mask.

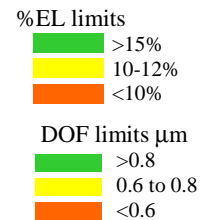
The DOF from XSEM analysis at best dose for all the reticles is shown in Table 1 and the Exposure Latitude from XSEM analysis at best focus for the binary, 6% and 33% mask is shown in Table 2. We have excluded results from the 20% mask, as they did not confirm certain predictions. This may be due to the CD errors observed on this mask. The dense 1:1 features do not resolve with the binary, 6%, 20% or 33% attenuated masks with conventional illumination. This may be related to the resolution limit of ( $\lambda/NA$ ). The binary mask showed poor depth of focus (less than 0.6μm at 6% Exposure Latitude) for the dense and isolated pitches. For the semi-dense pitches its performance was reasonable but less than 0.75μm DOF. For the 6% mask, the DOF performance improves up to 45% over the binary. For the 33% mask DOF improvement up to 35% is seen over the 6% mask. There is not much improvement in the isolated line performance with the attenuated PSM over the binary, but 6% better than 20% better than 33% attenuated PSM. From Table 2 it is seen that Exposure Latitude gets better with higher transmission and improvement in EL for isolated features is seen.

**Table 1 DOF at best Dose for 160nm features, with 0.6NA and 0.8σ**

Line/Space	BINARY	6%ATT	33%ATT
0.16/0.20	0.45	0.80	0.90
0.16/0.24	0.65	0.60	>>1.04
0.16/0.30	0.70	0.65	1.00
0.16/0.34	0.73	0.82	0.90
0.16/0.42	0.72	0.75	0.70
0.16/0.80	0.50	0.75	0.80
0.16/--/	0.50	0.55	0.70

**Table 2 Exposure Latitude at best focus for 160nm features, with 0.6NA and 0.8σ**

Line/Space	BINARY	6%ATT	33%ATT
0.16/.20	10.0	8.0	17.0
0.16/0.24	9.5	12.0	17.5
0.16/0.30	12.0	10.0	15.0
0.16/0.34	6.0	9.0	15.0
0.16/0.42	6.0	9.0	18.0
0.16/0.80	6.0	12.0	15.0
0.16/--/	6.0	14.0	15.0



Across Pitch bias (Figure 4): Excluding pitches below  $\lambda/NA$  for both 6% and 33% mask is the same. The TIR is about 27nm. The CD through pitch behavior for the 6% and 33% is same as the binary mask.

Linearity (Figure 5): Isolated features linear to 0.14μm for all masks and may be linear below. Dense features linear to 0.14μm for the 20% and 33% mask, and may not be below. Larger dense and isolated features are not linear beyond 0.3μm, except for the dense 6% att. feature. Note: smallest feature on mask 0.14μm and largest 0.30μm

The Process windows and its output for the 6% att. mask for all pitches except the 1:1 are shown in Figures 6-8. Individual DOF improved by 10-40% for the 6% att. Mask over the binary mask. Including duty cycles from 1.5 to isolated, 0.45μm overlapping DOF (ODOF) is obtained at 6%EL. Thus OPC would be required for overlap of dense features (pitch less than 240) with the pitches larger than 240nm. For the 20% mask, for pitches above 240 nm a DOF from 0.5 –1.1 μm is seen in Figures 9-11. No process window overlap is seen between features. Excluding isolated features an ODOF of 0.5μm can be obtained. Isolated features can be overlapped with the dense by applying scattering bar OPC (5).

The 33% attenuated dense and semi-dense features showed a DOF of about 0.7-1.0μm. No ODOF between pitches with this transmission (Figures 12-14). The 33% mask does show the EL to be highest for the isolated features. The performance improvement of isolated lines is least, but 33% slightly better than 6% slightly better than binary.

It was observed that the 33 %T PSM tends to required higher exposure dose than the 20%. The 20%, in turn, required higher dose over 6%. The higher transmission inherently produces a better resolution or higher aerial image contrast (3). Data confirmed the case between 33% and 6% but not the 20%. This may be due to the mask CD's being smaller on the 20% mask.

We can make an observation with conventional illumination that as transmission increases the ODOF reduces due to high contrast on the isolated features.

## **3.2. Annular Illumination, $\sigma_i = 0.6$ and $\sigma_o = 0.8$**

### **3.2.1. Process Window Results**

In order to increase the DOF of dense features, annular illumination is used with a 0.6 inner sigma and a 0.8 outer sigma. The choice of the annulus was limited by the tool configuration. The results of the 6% mask in Figures 15-17 showed features with duty cycles less than 2 to have a good DOF, from 0.7-1.1 $\mu\text{m}$ . Isolated features performance is below the specification of 0.6 $\mu\text{m}$  DOF at 6%. Loss of Exposure Latitude is observed with off-axis illumination. Loss of EL is made up in the gain in DOF for dense features. With off-axis illumination, proximity effects were enhanced. No overlap of process windows was observed between pitches for any transmission. For 6% the ODOF reduced from 0.45  $\mu\text{m}$  to 0.0  $\mu\text{m}$ . The 33% attenuated mask (Figures 18-20) when imaged with annular illumination showed 0.8-1 $\mu\text{m}$  DOF for features with duty cycles up to 3. For Isolated features the performance was marginal, but still better than 6% mask. Better resolution was observed with the 33% mask, 1:1 features were well resolved than with the 6% mask. Simple 1-D OPC on dense features and scattering bar type OPC can cause process windows to overlap.

### **3.2.2. Pattern Fidelity through Defocus**

Figure 21 shows a "Modified Brunner structure" for the 6% and 33% mask for best dose and focus and at best dose and 0.2mm defocus. Less proximity bias is seen on the 33% mask than on the lower transmission mask. Also the dense-iso bias holds better through defocus with higher transmission. Pattern fidelity of the Brunner structures on the mask through defocus showed more robustness with the higher transmission, which agrees with past simulation studies (3). This indicates higher transmission requires less aggressive OPC.

## **4. Addressing Mask Fabrication :**

### **4.1. Material availability**

High transmission blanks are not in production today. Though an increase in demand has been seen over the past year for 20%-attenuated material. This will be no issue about material if there is enough demand and a consensus on the transmission in the semiconductor industry. However high transmission may be an issue in some other areas as noted below.

### **4.2. Defect Inspection**

Today inspection capability at 365nm is in manufacturing, inspection at actinic wavelength in development. High transmission mask inspection not at actinic wavelength may cause problems. Lack of contrast between the attenuated material and glass and the attenuated material and chrome due to the high transmission makes it difficult to inspect the HIT att. PSM. Inspection capability of high transmission (18%) MoSi on quartz has been demonstrated (6). A critical inspection is that of the tri-tone layer i.e. chrome on the MoSi; especially when chrome is used for sidelobe suppression in contact hole applications. Attempts at inspection of the tri-tone reticles failed at 363nm wavelength. Currently, Tri-tone inspection algorithms are in a development state by some vendors.

### **4.3. Repair**

Repair of opaque and clear defects using Focus Ion Beam techniques has been demonstrated for attenuated masks. Post repair effects such as Gallium stains and river bedding are a concern. A variety of techniques such as gas assisted etching (7), biased repair method (8) or edge wall with wet etching (9) help restore the full process window. There should be no additional issues with repair of High transmission masks. A different stoichiometry and thickness of the material may require some minor process adjustment in repair techniques.

#### **4.4. Tri-tone Fabrication**

Tri-tone masks require the additional chrome layer on top of the attenuating material to have tight tolerances. The CD and overlay of chrome to the attenuating layer must be well controlled. Overlay tolerances specified by the mask makers today (approx. 40-50nm) is not sufficient for critical area chrome shields (i.e. chrome shields for sidelobe suppression), chrome scattering bars or rims that are not self-aligned. The overlay of the layer needs to be tightened to less than 25nm, for no adverse effect due to the misalignment on process windows.

#### **5. Summary:**

Dense features benefit most from high transmission. Largest with 33% mask, about 1 $\mu$ m. For duty cycles larger than 1:3 the performance of 33% slightly better than 6%, 6% slightly better than binary. Exposure Latitude increases as %Transmission increases. Proximity effect TIR (total indicated range) with conventional illumination same for all transmissions. Resist profiles had smooth sidewalls greater than 87°. Exposed and small (<0.3 $\mu$ m) unexposed areas were not affected by the transmitted portion of the light through the attenuated areas, Figure 22.

#### **ACKNOWLEDGEMENTS**

International Sematech, Optical Extension program manager Gilbert Shelden and the Optical Extension Technical steering committee for their support. Fung Chen from ASML masktools for helpful discussions.

#### **REFERENCES**

1. Attenuated phase-shifting mask in combination with off-axis illumination: a way towards quarter micron deep-UV lithography for random logic applications, *Microelectronic Engineering*, Vol 23, 133 (1994)
2. Process capability analysis of DUV Alternating PSM and DUV Attenuated PSM Lithography for 100nm Gate Fabrication, Keeho Kim, et al, *SPIE Vol. 4000, Optical Microlithography XIII*, 2000
3. Assessment of a Hypothetical roadmap that extends optical Lithography over the 70nm technology node, J. S. Petersen, et al., *SPIE Vol. 3546*, p. 288, Annual BACUS Symposium on Photomask Technology, 12/1998
4. Design of optical interference coatings, Thelen Alfred, McGraw-Hill, c1989
5. Imaging contrast improvement for 160-nm line features using subresolution assist features with binary, 6% ternary attenuated phase-shift mask with process-tuned resist, Kachwala, Nishrin et al; *Proc. SPIE Vol. 3679*, p 55-67, *Optical Microlithography XII*, 07/1999
6. High transmission PSM inspection sensitivity, Chun-Hung Wu et al; *Proc. SPIE Vol. 3873*, p 117-126, Annual BACUS Symposium on Photomask Technology, 09/1999
7. H. Nakamura, et al, *Jpn. J. Appl. Phy Vol. 31*, 1992, p. 3055
8. Focused Ion Beam Repair of Embedded Phase Shift Masks, Z. Cui et al, *SPIE Vol. 3051*, p 276, *Optical Microlithography X*, 07/1997
9. M. Matsumoto, et al, *SPIE Vol. 3096, Photomask and X-Ray Mask Technology IV*, 8/1997

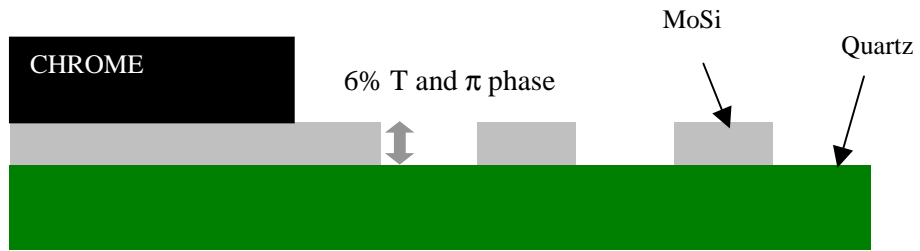


Figure 1: a) Tri-tone 6% attenuated PSM

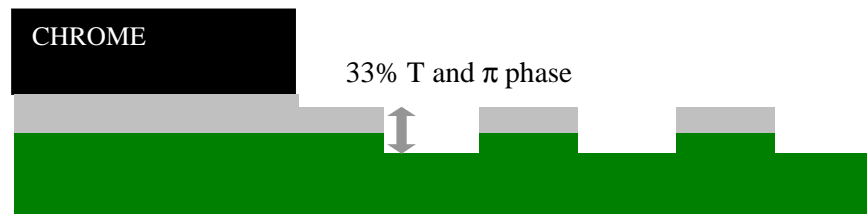


Figure 2: High transmission tri-tone PSM made by reducing the MoSi thickness, etch of the quartz for  $\pi$  phase difference

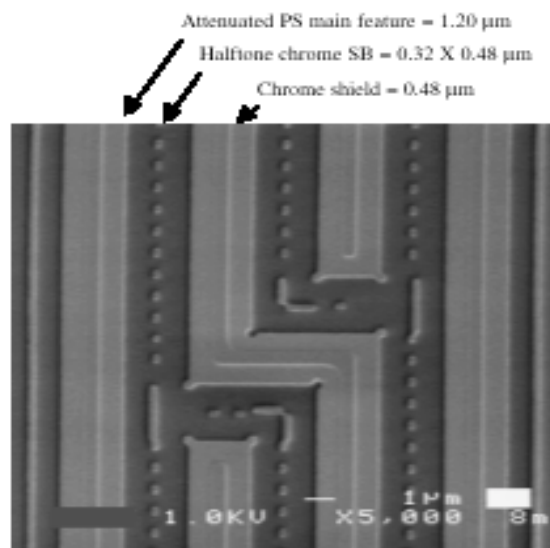


Figure 3 : SEM view of the tritone mask, showing the chrome shields on top of the MoSi

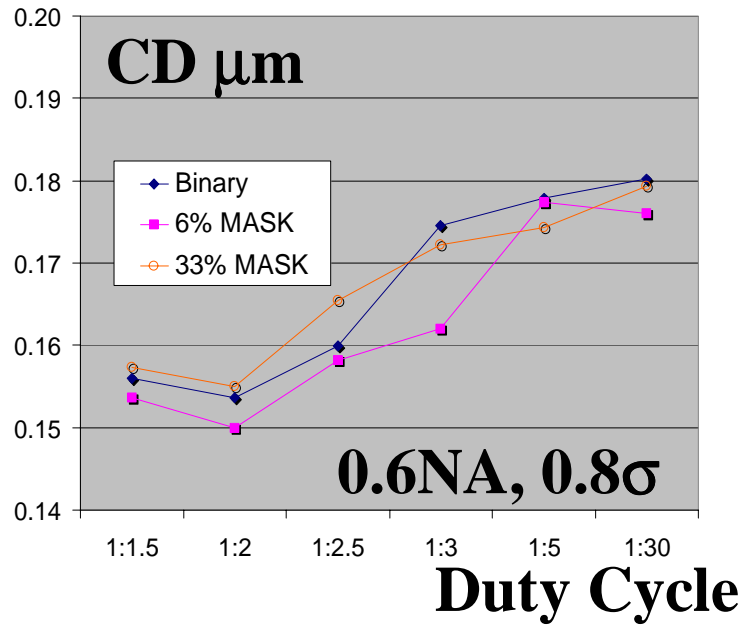


Figure 4: Proximity Effect with conventional illumination, NA=0.6 and  $\sigma=0.8$  for pitches above  $\lambda/\text{NA}$

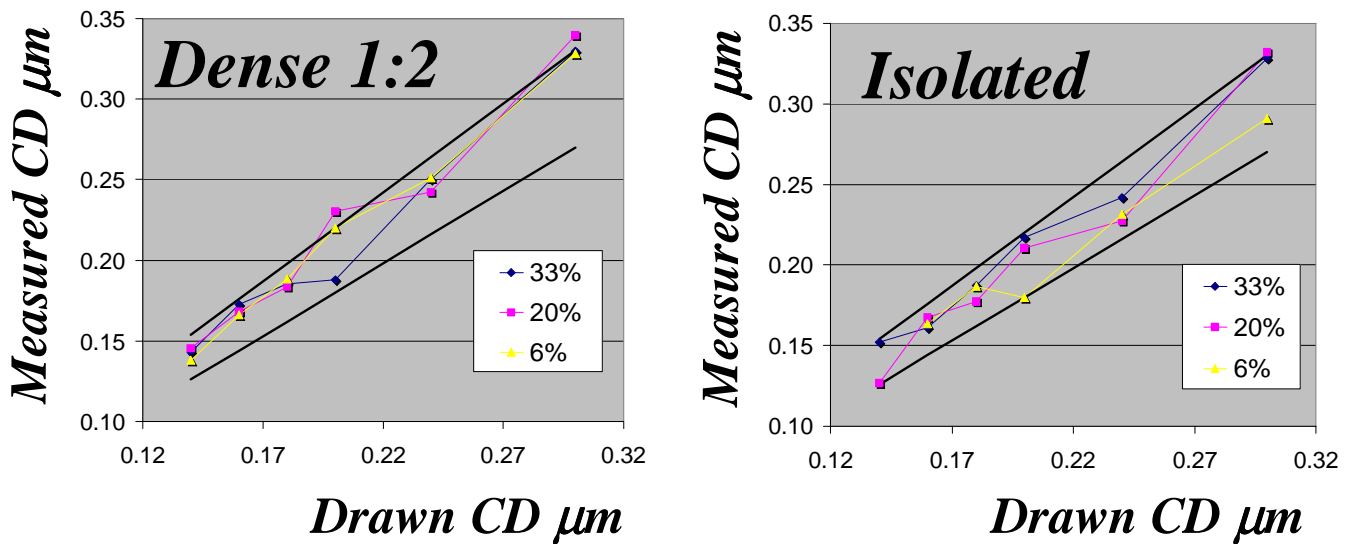
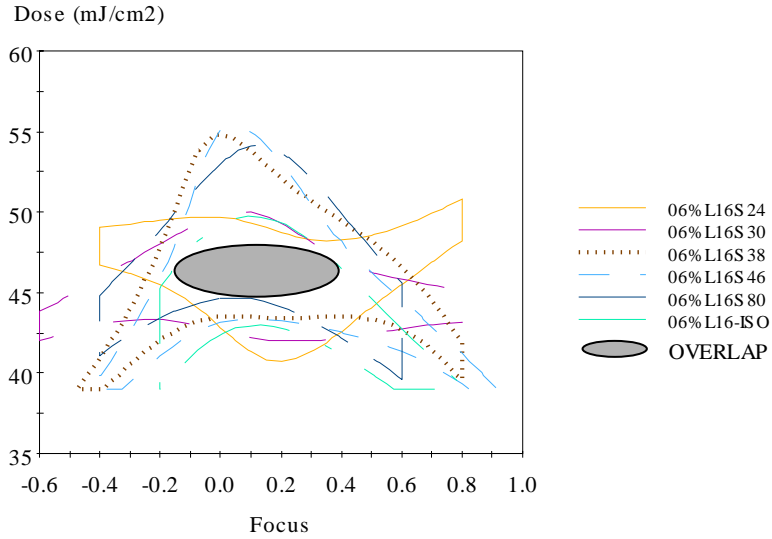
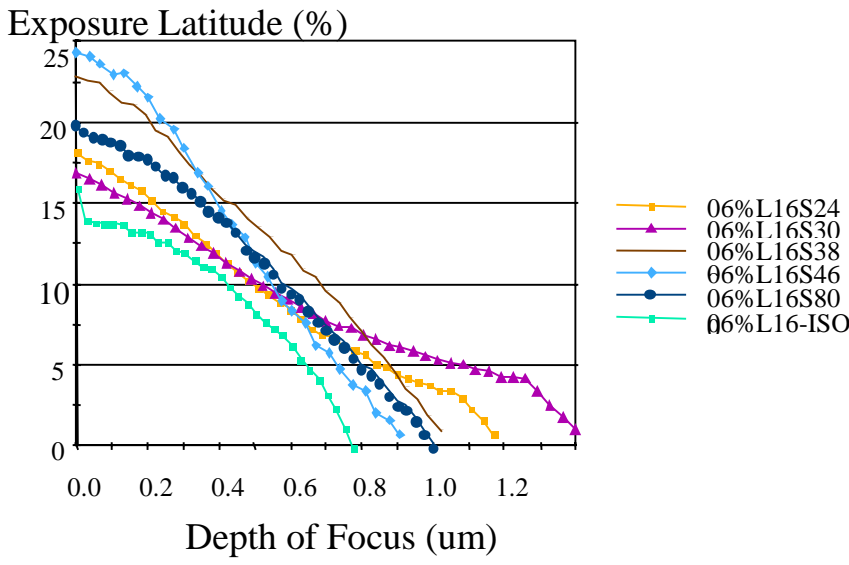


Figure 5: Linearity of dense and Isolated features with conventional Illumination, NA=0.6 and  $\sigma=0.8$



**Figure 6: Process Windows for 6% attenuated mask, NA=0.6 and  $\sigma=0.8$**

SPACE	DOF@6 %EL
<b>0.20</b>	<b>0.56</b>
<b>0.24</b>	<b>0.75</b>
<b>0.30</b>	<b>0.91</b>
<b>0.46</b>	<b>0.67</b>
<b>0.80</b>	<b>0.83</b>
<b>1.60</b>	<b>0.60</b>



**Figure 8: Exposure Latitude vs. DOF for 6% attenuated mask, NA=0.6 and  $\sigma=0.8$**

**Figure 7: DOF for 6% attenuated mask from process window with NA=0.6 and  $\sigma=0.8$**

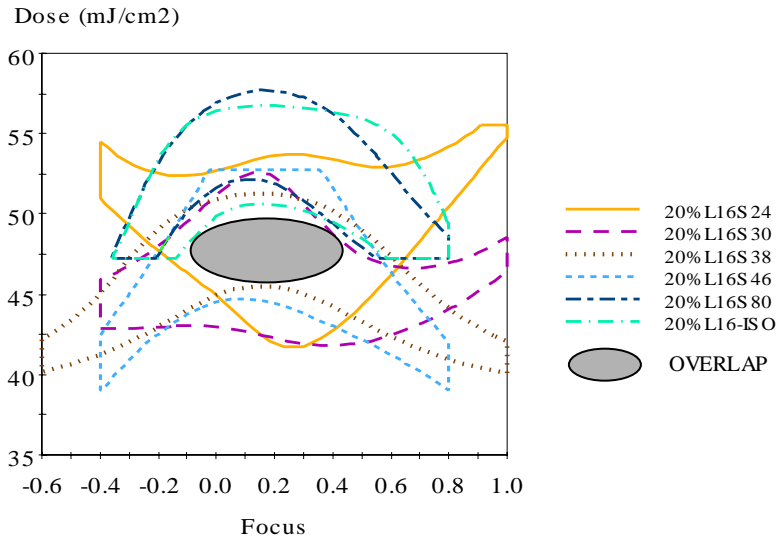


Figure 9: Process Windows for 20% attenuated mask, NA=0.6 and  $\sigma=0.8$ , Excluding isolated features ODOF is  $0.5\mu\text{m}$  at 6% EL

SPACE	DOF@ 6%EL
<b>0.20</b>	<b>0.54</b>
<b>0.24</b>	<b>1.00</b>
<b>0.30</b>	<b>1.10</b>
<b>0.46</b>	<b>0.72</b>
<b>0.80</b>	<b>0.52</b>
<b>1.16</b>	<b>0.70</b>

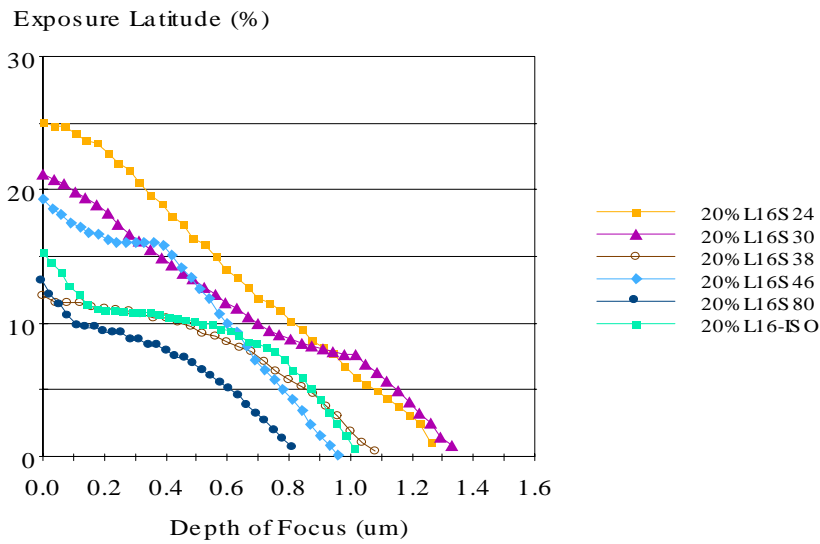
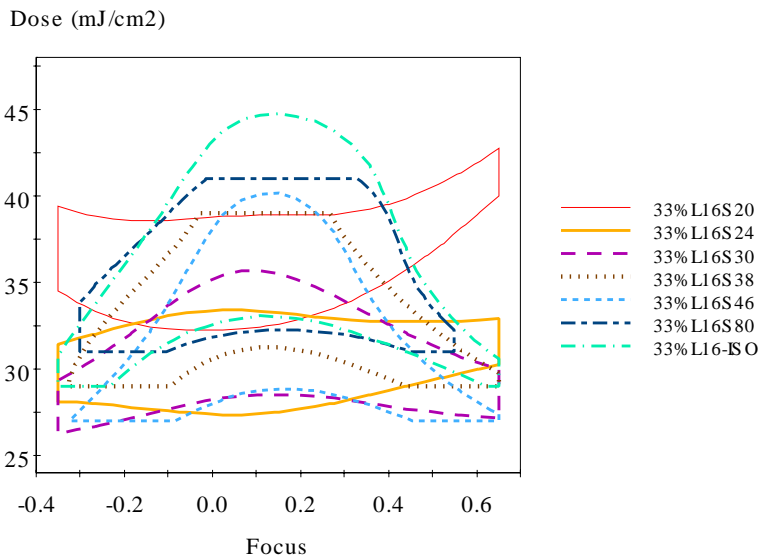


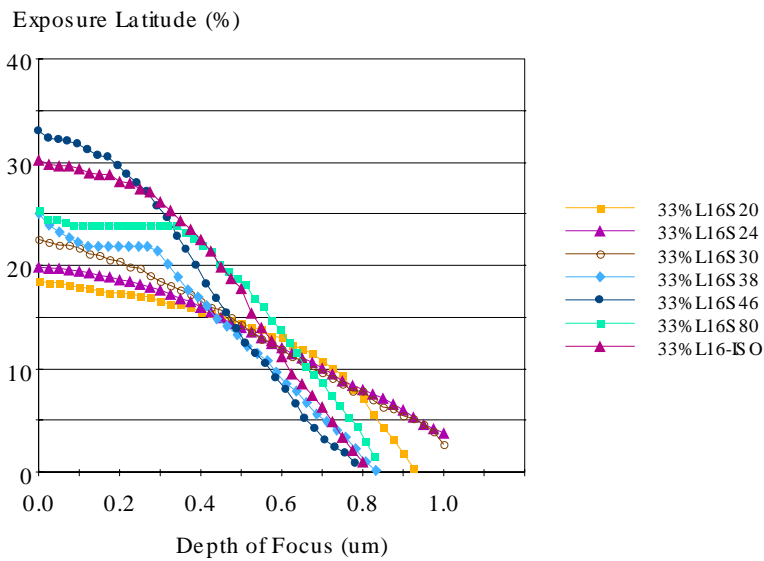
Figure 11 Exposure Latitude vs. DOF for 20% attenuated mask, NA=0.6 and  $\sigma=0.8$

Figure 10: DOF for 20% attenuated mask with NA=0.6 and  $\sigma=0.8$



**Figure 12: Process Windows for 33% attenuated mask, NA=0.6 and  $\sigma=0.8$  with UV6 process**

SPACE	DOF@6%EL
<b>0.20</b>	<b>0.80</b>
<b>0.24</b>	<b>0.90</b>
<b>0.30</b>	<b>0.85</b>
<b>0.38</b>	<b>0.65</b>
<b>0.46</b>	<b>0.60</b>
<b>0.80</b>	<b>0.75</b>
<b>1.60</b>	<b>0.70</b>



**Figure 14: Exposure Latitude vs. DOF for 33% attenuated mask, NA=0.6 and  $\sigma=0.8$  with UV6 process**

**Figure 13: DOF for 33% attenuated mask with NA=0.6 and  $\sigma=0.8$ , UV6 process**

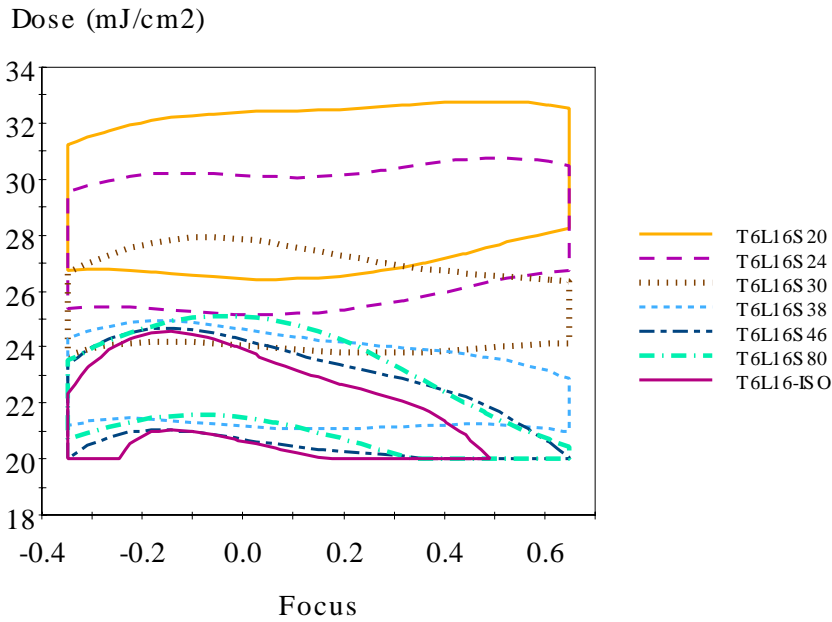


Figure 15: Process Windows for 6% attenuated mask, NA=0.6 and annulus 0.6/0.8, with UV6 process

SPACE	DOF@10 %EL
<b>0.20</b>	<b>0.98</b>
<b>0.24</b>	<b>0.98</b>
<b>0.30</b>	<b>0.70</b>
<b>0.46</b>	<b>0.55</b>
<b>0.80</b>	<b>0.53</b>
<b>1.60</b>	<b>0.38</b>

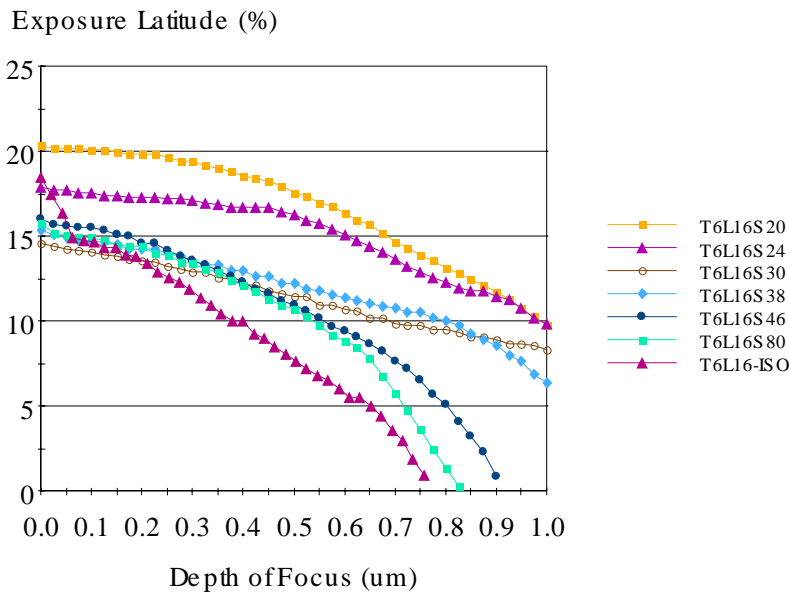


Figure 17: Exposure Latitude vs. DOF for 6% attenuated mask, NA=0.6 and annulus 0.6/0.8 with UV6 process

Figure 16: DOF for 6% attenuated mask with NA=0.6 and annulus 0.6/0.8, with UV6 process

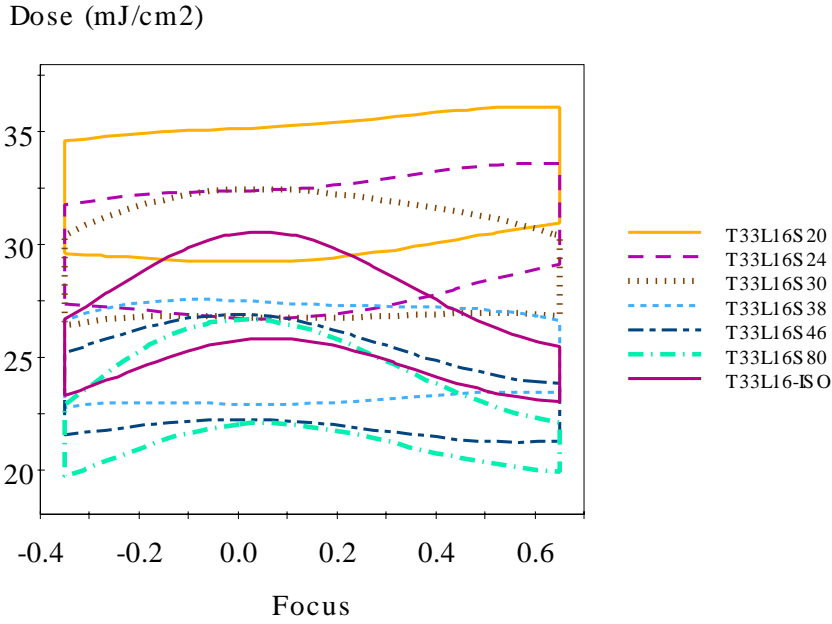


Figure 18: Process Windows for 33% attenuated mask, NA=0.6 and annulus 0.6/0.8, with UV6 process

SPACE	DOF@10%EI
<b>0.20</b>	<b>1.00</b>
<b>0.24</b>	<b>0.90</b>
<b>0.30</b>	<b>1.00</b>
<b>0.38</b>	<b>1.00</b>
<b>0.46</b>	<b>0.78</b>
<b>0.80</b>	<b>0.60</b>
<b>1.60</b>	<b>0.53</b>

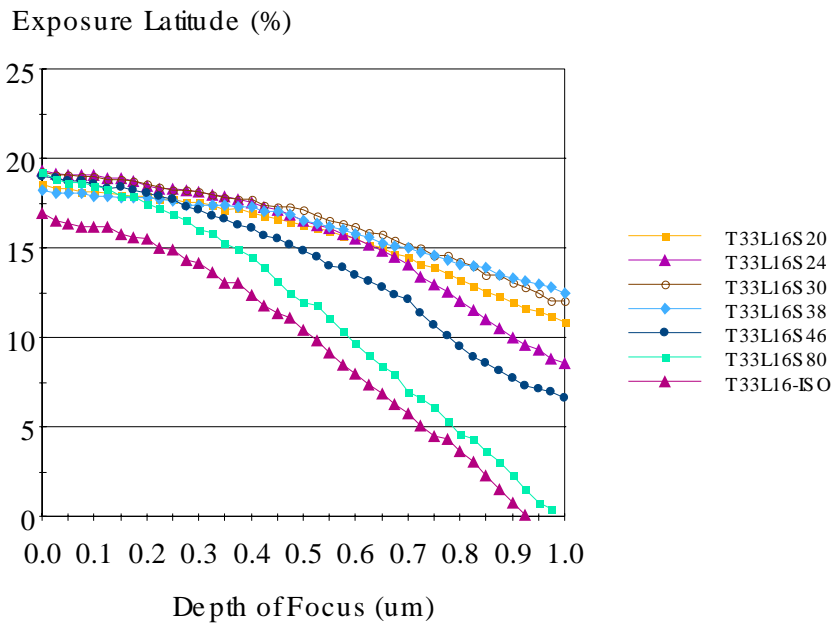


Figure 20: Exposure Latitude vs. DOF for 33% attenuated mask, NA=0.6 and annulus 0.6/0.8, with UV6 process

Figure 19: DOF for 33% attenuated mask with NA=0.6 and annulus 0.6/0.8, with UV6 process

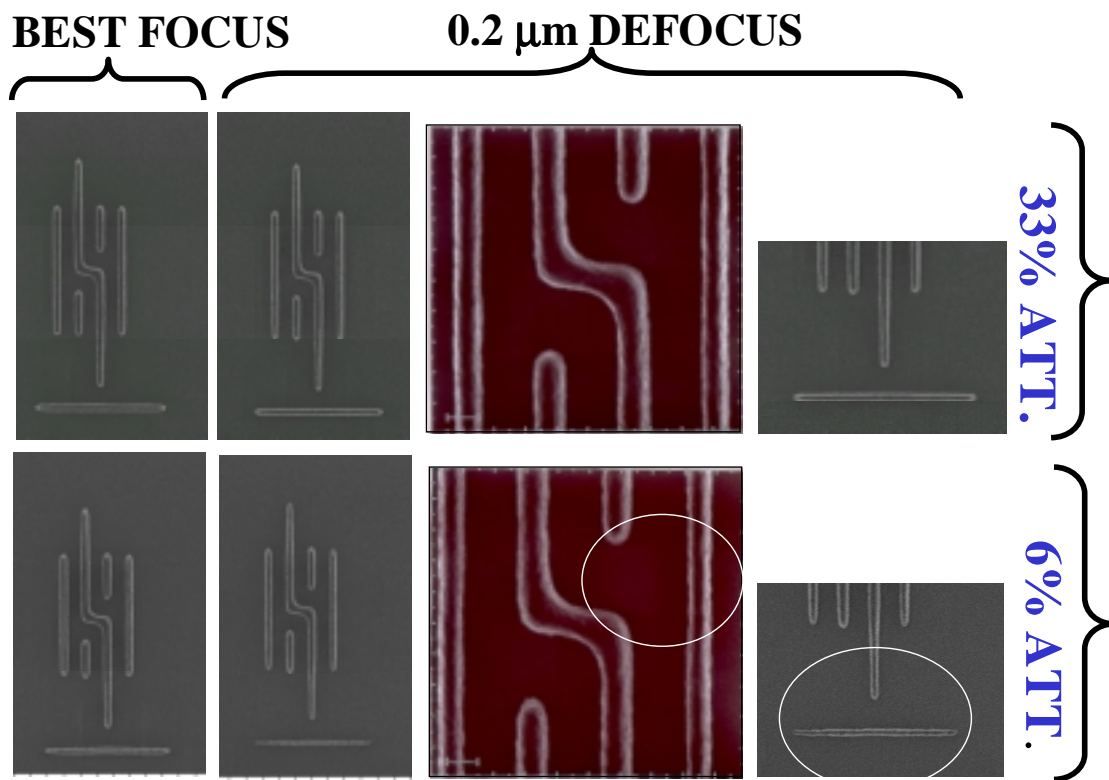


Figure 21: Pattern Fidelity of 6% and 33% attenuated masks through defocus

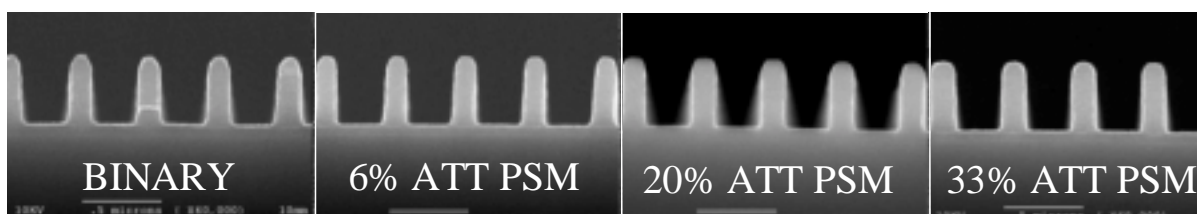


Figure 22: Resist profiles of Binary, 6%, 20% and 33% masks for 1:2 160nm features with conventional illumination, NA=0.6 and  $\sigma=0.8$